Black-hole horizon in the Dirac semimetal Zn_{2}In_{2}S_{5}

Huaqing Huang, Kyung-Hwan Jin, and Feng Liu

Phys. Rev. B **98**, 121110 — Published 26 September 2018

DOI: 10.1103/PhysRevB.98.121110

Black hole horizon in a Dirac semimetal $Zn_2In_2S_5$

Huaqing Huang,[1] Kyung-Hwan Jin,[1] and Feng Liu[1,2]

[1] *Department of Materials Science and Engineering, University of Utah, Salt Lake City, Utah 84112, USA*

[2] *Collaborative Innovation Center of Quantum Matter, Beijing 100084, China*

(Dated: September 14, 2018)

Recently, realizing new fermions, such as type-I and type-II Dirac/Weyl fermions in condensed matter systems, has attracted considerable attention. Here we show that the transition state from type-I to type-II Dirac fermions can be viewed as a "type-III" Dirac fermion, which exhibits unique characteristics, including a Dirac-line Fermi surface with nontrivial topological invariant and critical chiral anomaly effect, distinct from previously known Dirac semimetals. Most importantly, we discover $Zn_2In_2S_5$ is a type-III Dirac semimetal, characterized with a pair of Dirac points in the bulk and Fermi arcs on the surface. We further propose a solid-state realization of the black-hole-horizon analogue in inhomogeneous $Zn_2In_2In_5$ to simulate black hole evaporation with high Hawking temperature. We envision that our findings will stimulate researchers to study novel physics of type-III Dirac fermions, as well as astronomical problems in a condensed matter analogue.

a. Introduction. The conception of topology[1–3] has been known in condensed matter physics since 1980s. However, it is until recently that we have witnessed an exponential growth in the field of topological phases of mater in the last decade; thanks to the introduction of concept of topological insulators (TIs)[4] and their proposition[5] and confirmation[6] in real material systems. This effective route to discovering TIs from theoretical conception to computational material proposition and to experimental confirmation has been followed by the discovery of other topological materials, such as topological crystalline insulator[7–9], Dirac semimetal[10–13], and most recently Wyel semimetal[14–17]. Depending on the geometry of Dirac cone, there are type-I and type-II Dirac/Weyl semimetals[18–22]. Interestingly, it has been shown that the interface or the "transition state" from type-I to type-II has distinctly different topological properties[23–25], which we will call it a "type-III" semimetal.Both type-I and type-II Dirac/Weyl semimetals have been experimentally confirmed in real materials[11,13,17,19,21]; however, so far type-III Dirac/Weyl semimetal remains a theoretical conception. Here, we will fill this outstanding gap by proposing a type-III semimetallic phase in $Zn_2In_2S_5$.

Topological semimetals host interesting new types of fermions as low-energy quasiparticles. They not only exhibit novel physical properties such as topological surface states[10–18], large linear magnetoresistance[26–28] and chiral anomaly[29–34], but also offer a versatile platform for simulating relativistic particles of high-energy physics as well as "new particles" that have no counterparts in high-energy physics. The type-III Dirac semimetal has been theoretically proposed for realizing a solid-state analogue of block hole horizon[23–25]. To this end, we will again fill the gap by devising a material platform, an inhomogeneous $Zn_2In_2S_5$, to simulate Hawking radiation at the black-hole horizon. Especially we suggest a high Hawking temperature associated with the analogous black-hole horizon in $Zn_2In_2S_5$ to ease the experimental observation, in contrast to the low Hawking temperature in previously proposed black-hole-horizon analogues.[35–39]

We will first highlight the key features of the type-III Dirac semimetals, including their unique Dirac-line Fermi surface with nontrivial topological invariant and critical chiral magnetic effect, in distinction from those of type-I and type-II Dirac semimetals. Then we will present evidence that $Zn_2In_2S_5$ is the first candidate material for realizing the type-III Dirac fermions. Based on effective Hamiltonian analysis and first-principles calculations, we show novel properties of $Zn_2In_2S_5$ including critical chiral magnetoresponse and Fermi arcs. Finally we will describe a solid-state realization of the black-hole-horizon analogue in inhomogeneous $Zn_2In_2S_5$, to simulate black hole evaporation with a relatively high Hawking temperature.

b. The concept of type-III Dirac/Weyl point. Topological Dirac and Weyl semimetals are characterized with fourfold and twofold linear band crossings at the Fermi level (the so-called Dirac and Weyl points), respectively. They can be further classified into two types by fermiology. The type-I Dirac/Weyl semimetals have a typical conical dispersion and point-like Fermi surface [Fig. 1(a)][10–13,16,17]. The type-II Dirac/Weyl semimetals have an overtilted cone-shape band structure, possessing both electron and hole pockets that contact at the type-II Dirac/Weyl point [Fig. 1(b)][18–22]. The type-III Dirac semimetal is distinct from both type-I and type-II semimetals.[41] As illustrated in Fig. 1(c), the type-III Dirac point is also a protected band crossing point, but appears at the contact of a line-like Fermi surface. Unlike Fermi surfaces of other topological semimetals, such a unique line-like Fermi surface, so-called Dirac line, is protected by a topological invariant which is an integer only for the relatively rare Dirac line.

Since a Dirac point can be viewed as the merge of a pair of Weyl points with opposite chirality, we start by considering a general 4×4 Hamiltonian composed of two

TABLE I. Comparison among three types of Dirac semimetals.

	Type-I	Type-II	type-III
Dispersion	Dirac cone	Overtilted Dirac cone	Critical Dirac cone
Fermi surface	Point-like	Electron & hole pockets	Dirac line (with $N_2 = 1$)
DOS(E_F)	Vanishing	Parabolic peak	Finite
Surface Fermi Arc	✓	✓	✓
Chiral anomaly	Along all direction	Anisotropic, inside a cone region[40]	Except for the critical plane [41]
Black hole analogue	Outside	Inside	Horizon
Typical materials	Na_3Bi[10], Cd_3As_2[12]	$PtTe_2$[20,21], VAl_3[22]	$Zn_2In_2S_5$ (this work)

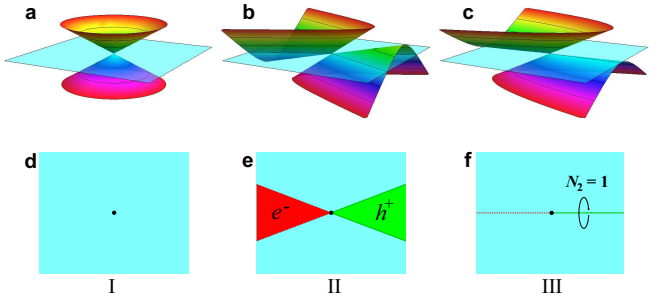

FIG. 1. (a) Type-I Dirac point with a point-like Fermi surface. (b) Type-II Dirac point is the contact point between electron and hole pocket. (c) Type-III Dirac point appears as the touching point between Dirac lines. The Dirac line is described by the topological invariant $N_2 = 1$. The light blue semitransparent plane corresponds to the position of the Fermi level, and the black solid/dashed lines mark the boundary of hole/electron pockets. (d)-(f) Fermi surfaces of three types of Dirac semimetals.

2×2 Hamiltonian describing Weyl points for simplicity,

$$H(\mathbf{k}) = \begin{pmatrix} h(\mathbf{k}) & 0 \\ 0 & h^*(-\mathbf{k}) \end{pmatrix} \tag{1}$$

with

$$h(\mathbf{k}) = \mathbf{v} \cdot \mathbf{k}\sigma_0 + \sum_{i,j} k_i A_{ij} \sigma_j, \tag{2}$$

where σ_j are Pauli matrices and σ_0 is the identity matrix. The energy spectrum of a Weyl point is $E_\pm(\mathbf{k}) = \sum_i v_i k_i \pm \sqrt{\sum_j \left(\sum_i k_i A_{ij}\right)^2} = T(\mathbf{k}) \pm U(\mathbf{k})$. It is well-known that if there exists a direction for which $T > U$, the band crossing point is a type-II Dirac point, otherwise it is type-I. If and only if for a particular direction $\hat{k}$ that $T(\hat{k}) = U(\hat{k})$, but $T(\hat{k}) < U(\hat{k})$ for other directions, the Dirac points are connected by a line-like Fermi surface as for the type-III Dirac semimetal. It is distinctively different from the type-I point-like Fermi surface or the type-II hyperbolic Fermi surface (coexistence of electron and hole pockets). The Dirac line is protected by the combination of topology and symmetry, and can be described by a topological invariant[24],

$$N_2 = \frac{1}{4\pi i} \mathrm{Tr}[K \oint_c dl h(\mathbf{k})^{-1} \partial_l h(\mathbf{k})], \tag{3}$$

where C is a contour enclosing the Dirac line in momentum space. Here the symmetry operator K depends on the direction of the Dirac line; for the Dirac line along k_z direction, $K = \sigma_z$ (see Supplemental Material[42]). The topological invariant is actually a winding number of phase around the line, and it stabilitzes the Dirac line in the sense that the integral is integer, $N_2 = 1$ only for type-III semimetal. The Dirac line with a nonzero winding number is an analogue of the vortex line in superfluids[37].

Interestingly, the Dirac cone band structure is tilted exactly with a flat band without dispersion along the particular direction of $E_n(\mathbf{k}) = 0$, which serves as a characteristic feature of type-III Dirac cone. The apparent qualitative distinction between the Fermi surface and band dispersion of the type-III and those of other types of Dirac cones lead to significant differences in their physical properties, such as critical chiral magnetoresponse[40]. In particular, the chiral anomaly appears in a type-III Dirac semimetal for almost all the directions of magnetic field. Only when the direction of magnetic field is exactly perpendicular to the tilt, the Landau levels collapse due to open semiclassical cyclotron orbit having no chiral zero mode (see Supplemental Material[42]). We note that also different from Type-I and -II Dirac fermions which exist over a wide range of "phase" space (tilting angle), the type-III exists only at a fixed tilting angle so that in this sense it is less robust than the Type-I and -II.

Furthermore, the type-III Dirac semimetal can also be viewed as the critical state of Lifshitz transition between type-I and type-II[24]. It was investigated recently as a solid-state realization of black-hole-horizon analogue based on inhomogeneous topological semimetals[23–25]. So far, however, no material system is known to be a type-III Dirac semimetal. Next, we will demonstrate $Zn_2In_2S_5$ to be the first type-III Dirac semimetal, and how to realize its black-hole-horizon analogue.

c. The type-III Dirac semimetal state in $Zn_2In_2S_5$. $Zn_2In_2S_5$ has a layered structure consisting of nonuple layers stacked together along the z-direction[42]. Each nonuple layer consists of two In and two Zn layers which are sandwiched by S layers alternately, and every In or Zn atom lies in the center of a terahedron or octahedron of S atoms. The coupling is strong between atomic layers within the nonuple layer but much weaker between adjacent nonuple layers. By different stacking of these basic building blocks, two kinds of $Zn_2In_2S_5$ arise, i.e., AB-

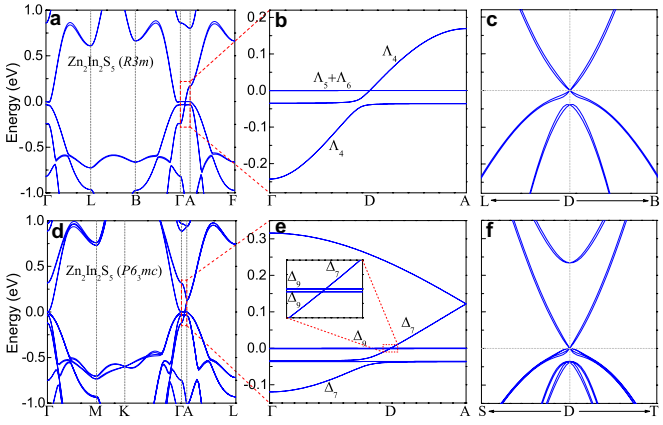

FIG. 2. Band structures of (a)-(c) $Zn_2In_2S_5(R3m)$ and (d)-(f) $Zn_2In_2S_5(P6_3mc)$. (b) and (e) The zoom-in band structures along Γ-A of $Zn_2In_2S_5(R3m)$ and $Zn_2In_2S_5(P6_3mc)$, respectively. (c) and (f) The in-plane band dispersions around the Fermi level of $Zn_2In_2S_5(R3m)$ and $Zn_2In_2S_5(P6_3mc)$, respectively.

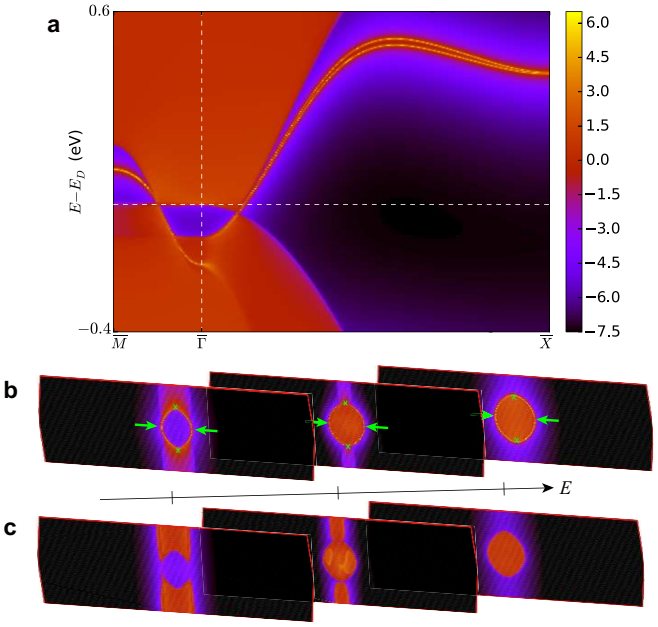

FIG. 3. (a) The projected surface density of states for the (100) surface of $Zn_2In_2S_5(R3m)$ where the nontrivial topological surface states originating from the surface projection of bulk Dirac point are clearly visible. (b) and (c) Constant energy contours of the (100) surface and the bulk at $E = E_F - 25$, E_F and $E_F + 25$ meV, respectively. The green arrows and crosses mark two pieces of Fermi arcs and the surface projection of bulk Dirac points, respectively.

stacked hexagonal structure with $P6_3mc$ symmetry and ABC-stacked rhombohedral structure with $R3m$ symmetry.

We first calculated the band structure of $Zn_2In_2S_5$. As shown in Fig. 2(a) and 2(d), there are flat bands along the Γ-A direction near the Fermi level. Meanwhile, another band disperses upward crossing the flat bands in between Γ and A. The upward dispersive band crosses with the upper flat band but avoids crossing with the lower flat band [Fig. 2(b) and 2(e)]. The band crossings occur in both materials, because the two crossed bands belong to different irreducible representations of the crystal symmetry group. For $Zn_2In_2S_5(R3m)$, the two bands belong to 2D Λ_4 and 1D Λ_5 /Λ_6 representations, respectively, as distinguished by C_{3v} symmetry around the k_z axis. The different representation prohibits hybridization between them, resulting in a pair of 3D Dirac points at $\pm(0.254, 0.254, 0.254)$ (in units of $2\pi/a$). For $Zn_2In_2S_5(P6_3mc)$, the upper flat band and the upward dispersive band belong to 2D Δ_9 and Δ_7, respectively, of the C_{6v} symmetry. One unique feature of the $P6_3mc$ structure is that there are actually adjacent double Dirac points $(0, 0, \pm 0.306)$ and $(0, 0, \pm 0.308)$ [in units of $(2\pi/a, 2\pi/a, 2\pi/c)$] with an energy difference of 1.0 meV. This is because there are actually two flat Δ_9 bands that are close to each other but not exactly degenerate [see inset of Fig. 2(e)]. Since neither $R3m$ nor $P6_3mc$ structure has inversion symmetry, these Dirac semimetals have fourfold degenerate Dirac points, but with splitting of in-plane band dispersions away from Dirac points [Fig. 2(c) and 2(f)]. This is an unique feature of $Zn_2In_2S_5$, which is different from other Dirac semimetals that require both time-reversal and inversion symmetries. Additionally, we also investigate the strain effect on the electronic structure and found that the position of type-III Dirac points in the k_z axis can be effectively tuned by external strain. As the two structures share similar electronic properties, we take $Zn_2In_2S_5(R3m)$ as an example hereafter.

To further reveal the nature of the type-III Dirac points, we fit first-principles results to a low-energy effective model[42]. Neglecting the insignificant tiny splitting induced by inversion symmetry breaking, the quasiparticles are described by a pair of Weyl Hamiltonian in the vicinity of one Dirac point,

$$h^c_{\pm} = c_{\perp}(k_x\sigma_x \pm k_y\sigma_y) + c_{\parallel}\delta k_z\sigma_z + v\delta k_z\sigma_0, \qquad (4)$$

where $\delta k_z = k_z - k^c_z$, with $k^c_z = 0.102$ Å^{-1}. The parameters $c_{\perp} = 2.29$ and $v = -c_{\parallel} = 1.36$ eVÅ, indicating that there exists a flat band along $\hat{k}_z$ direction. It is straightforward to derive the topological invariant using $K = \pm\sigma_z$ in Eq. (3) and find that $N_2 = 1$. We thus conclude that $Zn_2In_2S_5$ is a type-III Dirac semimetal.

The topological nature of the type-III Dirac point in $Zn_2In_2S_5$ is also confirmed by calculating the $\mathbb{Z}_2$ topological invariants which are well-defined in the $k_z = 0$ and $k_z = \pi$ planes. For the $k_z = 0$ plane, $\mathbb{Z}_2 = 1$; while for the $k_z = \pi$ plane, $\mathbb{Z}_2 = 0$. Therefore, a band order inversion between Λ_4 and $\Lambda_5 + \Lambda_6$ bands must occur along the k_z direction [see Fig. 2(b)], resulting in a band gap closure at the Dirac point.

Topological surface states and Fermi arcs are expected to appear on side surfaces of $Zn_2In_2S_5$. Figure 3 shows

the projected surface DOS for the (100) surface of a semi-infinite $Zn_2In_2S_5(R3m)$ system. It is seen that the topological surface state emanates from one projection of bulk Dirac point on the (100) surface, as shown in Fig. 3(a). The Fermi surface contains two pieces of half-circle Fermi arcs, as shown in Fig. 3(b), touching at two singularity points where the surface projections of bulk Dirac points appear. Due to the flat Dirac-line Fermi surface, the shape of electron and hole pockets varies rapidly with the increasing chemical potential. All these characteristics should be experimentally observable by modern angle-resolved photoemission spectroscopy technique.

d. The black-hole horizon analogue. Now we discuss the possibility of realizing a solid-state analogue of black-hole horizon in $Zn_2In_2S_5$. So far, various black-hole analogues have been proposed[43], such as a sonic black hole for sound wave propagating in flowing liquid[35] and a black-hole/white-hole pair in superfluid Helium with a moving vierbein domain well[36,37]. In Eq. (4), the last term is the same as the Doppler shift for quasiparticles under a Galiean transformation to a moving frame of reference with a velocity v. In general relativity, a relativistic quasiparticle in 3+1 dimensional spacetime can be described by the line element $ds^2 = g_{\mu\nu}dx^\mu dx^\nu$, where $g_{\mu\nu}$ is the inverse (covariant) metric describing an effective curved spacetime in which the relativistic quasiparticles propagate[44]. To obtain a spacetime interpretation, we derive an effective covariant metric $g_{\mu\nu}$ according to Eq. (4)[42]:

$$g_{\mu\nu} = \begin{pmatrix} -(1-v^2/c_\parallel^2) & 0 & 0 & -v/c_\parallel^2 \\ 0 & 1/c_\perp^2 & 0 & 0 \\ 0 & 0 & 1/c_\perp^2 & 0 \\ -v/c_\parallel^2 & 0 & 0 & 1/c_\parallel^2 \end{pmatrix}, \qquad (5)$$

which has a similar form of the acoustic metric of Unruh's sonic black hole[35,43].

Now let's assume that the dragging velocity $v = v(z)$ depends on the spacial z coordinate in an inhomogeneous $Zn_2In_2S_5$ system, which can, in principle, be realized by controllable (tunable) structural distortion. As the metric has translation invariance in the x- and y-direction, for simplicity we make a dimension reduction to the 1+1 dimensional spacetime by ignoring the coordinates x and y. As a result, the corresponding linear element becomes

$$ds^2 = -\left(1 - \frac{v^2(z)}{c_\parallel^2}\right) d\tau^2 + \frac{dz^2}{c_\parallel^2 - v^2(z)}. \qquad (6)$$

By performing a coordinate transformation: $\tau = t + \int^z dz v(z)/(c_\parallel^2 - v^2(z))$, we obtain an effective line element that shares the same form of the radial part of the Schwarzschild line element for gravitational black holes[44]. Similar to the Schwarzschild metric which has a singularity at the Schwarzschild radius corresponding to an event horizon, the above matric also has a horizon (z_h), where the dragging velocity equals to the local "speed of light" for quasiparticles: $v(z_h) = \pm c_\parallel$. The corresponding "Newtonian gravitational field" at horizons is given by: $E_g(z_h) = \frac{v(z_h)}{c_\parallel^2}\left.\frac{dv}{dz}\right|_{z_h}$. According to the fitted parameters of Eq. (4), assuming $v(z) > -c_\parallel$ ($v(z) < -c_\parallel$) in the region $z > z_h$ ($z < z_h$), an inhomogeneous $Zn_2In_2S_5$ system can be derived (see Fig. 4). Hence all quasiparticles in the upper region ($z > z_h$) move upward, and cannot cross the $z = z_h$ plane, which indicates that this plane is the black-hole horizon. Consequently, the inner observers living in the lower region ($z < z_h$) cannot obtain any information from the upper region ($z > z_h$) if they can only use the relativistic quasiparticles for communication.

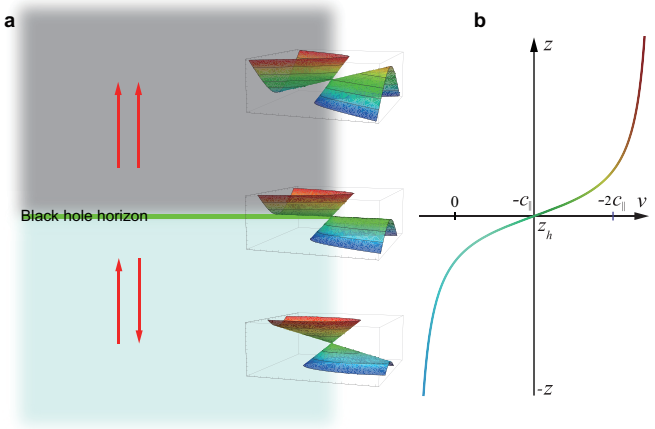

FIG. 4. (a) Schematic illustration of the solid-state analogue of black hole horizon in an inhomogeneous $Zn_2In_2S_5$ with controllable structural distortion. The red arrows indicate quasiparticle propagating directions in each region. (b) The dependence of the dragging velocity v on the z coordinate.

A black hole can slowly radiate away its mass by emitting a thermal flux at the horizon, as pointed out by Hawking[45]. The analogous model presented above not only suggests a new route to simulating an event horizon, but also facilitates the realization of the Hawking radiation analogue in dynamically inhomogeneous type-III Dirac semimetals. Although this model is static in equilibrium, the dissipation process right after the creation of the black hole horizon analogue is similar to the process of Hawking radiation[23–25]. The corresponding Hawking temperature can be determined by the "surface gravity" at the horizon $E_g(z_h)$[37,43]:

$$T_H = \frac{\hbar c_\parallel}{2\pi k_B} E_g(z_h) = \frac{\hbar}{2\pi k_B}\left.\frac{dv}{dz}\right|_{z_h}, \qquad (7)$$

where k_B and $\hbar$ are the Boltzmann and the reduced Planck constants, respectively. Obviously, T_H may reach high temperature as long as the gradient of the dragging velocity is sufficiently large across the horizon. As the dragging velocity v is a material-dependent parameter which can be effectively tuned by strain and chemical doping[46,47], a high value of T_H is expected in inhomogeneous $Zn_2In_2S_5$.

e. Discussion. In conclusion, many recently emerging condensed matter analogs of high-energy particles are

not real high-energy particles themselves, but quasiparticles of low-energy electronic excitations. But they have provided really interesting physics topics of study, which are of tremendous interests to both fields of condensed matter and particle physics. For the case we studied here, the causal structure of the type-III Dirac semimetal is identical to the causal structure of a black hole in the presence of fermions, although not the black hole itself. It is interesting to note that this analogy to black hole by electronic fluid is different from the ones made previously by neutral fluid[35], because quantum effects are encoded already through DFT calculations in the present case. So some form of analogous "Hawking radiation" will definitely occur. In addition, other novel astrophysical phenomena such as gravitational lensing effect[47], gravity wave[48], and cosmological constant problem[36] can also be explored in type-III Dirac semimetals.

ACKNOWLEDGMENTS

We thank Yong-Shi Wu and Jaakko Nissinen for helpful discussions. This work was supported by DOE-BES (Grant No. DE-FG02-04ER46148). The calculations were done on the CHPC at the University of Utah and DOE-NERSC.

[1] D. J. Thouless, M. Kohmoto, M. P. Nightingale, and M. den Nijs, Phys. Rev. Lett. **49**, 405 (1982).
[2] F. D. M. Haldane, Phys. Rev. Lett. **50**, 1153 (1983).
[3] J. Kosterlitz and D. Thouless, J. Phys. C **5**, L124 (1972); J. M. Kosterlitz and D. J. Thouless, *ibid.* **6**, 1181 (1973).
[4] C. L. Kane and E. J. Mele, Phys. Rev. Lett. **95**, 146802 (2005); **95**, 226801 (2005).
[5] B. A. Bernevig, T. L. Hughes, and S.-C. Zhang, Science **314**, 1757 (2006).
[6] M. König, S. Wiedmann, C. Brüne, A. Roth, H. Buhmann, L. W. Molenkamp, X.-L. Qi, and S.-C. Zhang, Science **318**, 766 (2007).
[7] L. Fu, Phys. Rev. Lett. **106**, 106802 (2011).
[8] T. H. Hsieh, H. Lin, J. Liu, W. Duan, A. Bansil, and L. Fu, Nat. Commun. **3**, 982 (2012).
[9] Y. Tanaka, Z. Ren, T. Sato, K. Nakayama, S. Souma, T. Takahashi, K. Segawa, and Y. Ando, Nat. Phys. **8**, 800 (2012); P. Dziawa, B. Kowalski, K. Dybko, R. Buczko, A. Szczerbakow, M. Szot, E. Łusakowska, T. Balasubramanian, B. M. Wojek, M. Berntsen, *et al.*, Nat. Mater. **11**, 1023 (2012); Y. Okada, M. Serbyn, H. Lin, D. Walkup, W. Zhou, C. Dhital, M. Neupane, S. Xu, Y. J. Wang, R. Sankar, *et al.*, Science **341**, 1496 (2013).
[10] Z. Wang, Y. Sun, X.-Q. Chen, C. Franchini, G. Xu, H. Weng, X. Dai, and Z. Fang, Phys. Rev. B **85**, 195320 (2012).
[11] Z. K. Liu, B. Zhou, Y. Zhang, *et al.*, Science **343**, 864 (2014); S.-Y. Xu, C. Liu, S. K. Kushwaha, *et al.*, **347**, 294 (2015).
[12] Z. Wang, H. Weng, Q. Wu, X. Dai, and Z. Fang, Phys. Rev. B **88**, 125427 (2013).
[13] M. Neupane, S.-Y. Xu, R. Sankar, *et al.*, Nat. Commun. **5**, 3786 (2014); Z. K. Liu, J. Jiang, B. Zhou, *et al.*, Nat. Mater. **13**, 677 (2014).
[14] A. Burkov, M. Hook, and L. Balents, Phys. Rev. B **84**, 235126 (2011).
[15] X. Wan, A. M. Turner, A. Vishwanath, and S. Y. Savrasov, Phys. Rev. B **83**, 205101 (2011).
[16] H. Weng, C. Fang, Z. Fang, B. A. Bernevig, and X. Dai, Phys. Rev. X **5**, 011029 (2015); S.-M. Huang, S.-Y. Xu, I. Belopolski, C.-C. Lee, G. Chang, B. Wang, N. Alidoust, G. Bian, M. Neupane, C. Zhang, *et al.*, Nat. Commun. **6**, 7373 (2015).
[17] S.-Y. Xu, I. Belopolski, N. Alidoust, M. Neupane, G. Bian, C. Zhang, R. Sankar, G. Chang, Z. Yuan, C.-C. Lee, *et al.*, Science **349**, 613 (2015); L. Yang, Z. Liu, Y. Sun, H. Peng, H. Yang, T. Zhang, B. Zhou, Y. Zhang, Y. Guo, M. Rahn, *et al.*, Nat. Phys. **11**, 728 (2015); B. Lv, N. Xu, H. Weng, J. Ma, P. Richard, X. Huang, L. Zhao, G. Chen, C. Matt, F. Bisti, *et al.*, **11**, 724 (2015).
[18] A. A. Soluyanov, D. Gresch, Z. Wang, Q. Wu, M. Troyer, X. Dai, and B. A. Bernevig, Nature **527**, 495 (2015).
[19] K. Deng, G. Wan, P. Deng, *et al.*, Nat. Phys. **12**, 1105 (2016).
[20] H. Huang, S. Zhou, and W. Duan, Phys. Rev. B **94**, 121117 (2016).
[21] M. Yan, H. Huang, K. Zhang, E. Wang, W. Yao, K. Deng, G. Wan, H. Zhang, M. Arita, H. Yang, Z. Sun, H. Yao, Y. Wu, S. Fan, W. Duan, and S. Zhou, arXiv:1607.03643 (2016).
[22] T.-R. Chang, S.-Y. Xu, D. S. Sanchez, W.-F. Tsai, S.-M. Huang, G. Chang, C.-H. Hsu, G. Bian, I. Belopolski, Z.-M. Yu, S. A. Yang, T. Neupert, H.-T. Jeng, H. Lin, and M. Z. Hasan, Phys. Rev. Lett. **119**, 026404 (2017).
[23] G. E. Volovik, JETP Lett. **104**, 645 (2016).
[24] G. E. Volovik, arXiv:1604.00849 (2016).
[25] G. E. Volovik, arXiv:1701.06435 (2017).
[26] A. A. Abrikosov, Phys. Rev. B **58**, 2788 (1998).
[27] C. Shekhar, A. K. Nayak, Y. Sun, M. Schmidt, M. Nicklas, I. Leermakers, U. Zeitler, Y. Skourski, J. Wosnitza, Z. Liu, *et al.*, Nat. Phys. **11**, 645 (2015).
[28] T. Liang, Q. Gibson, M. N. Ali, M. Liu, R. Cava, and N. Ong, Nat. Mater. **14**, 280 (2015).
[29] H. B. Nielsen and M. Ninomiya, Physi. Lett. B **130**, 389 (1983).
[30] Y. Wang, E. Liu, H. Liu, Y. Pan, L. Zhang, J. Zeng, Y. Fu, M. Wang, K. Xu, Z. Huang, *et al.*, Nat. Commun. **7**, 13142 (2016).
[31] J. Xiong, S. K. Kushwaha, T. Liang, J. W. Krizan, M. Hirschberger, W. Wang, R. Cava, and N. Ong, Science **350**, 413 (2015).
[32] C.-Z. Li, L.-X. Wang, H. Liu, J. Wang, Z.-M. Liao, and D.-P. Yu, Nat. Commun. **6**, 10137 (2015); H. Li, H. He, H.-Z. Lu, H. Zhang, H. Liu, R. Ma, Z. Fan, S.-Q. Shen, and J. Wang, **7**, 10301 (2016).
[33] C.-L. Zhang, S.-Y. Xu, I. Belopolski, Z. Yuan, Z. Lin, B. Tong, G. Bian, N. Alidoust, C.-C. Lee, S.-M. Huang, *et al.*, Nat. Commun. **7**, 10735 (2016); X. Huang, L. Zhao, Y. Long, P. Wang, D. Chen, Z. Yang, H. Liang, M. Xue, H. Weng, Z. Fang, X. Dai, and G. Chen, Phys. Rev. X **5**,

031023 (2015).
[34] H. Huang and F. Liu, Phys. Rev. B **95**, 201101 (2017).
[35] W. G. Unruh, Phys. Rev. Lett. **46**, 1351 (1981); Phys. Rev. D **51**, 2827 (1995); M. Visser, Class. Quantum Grav. **15**, 1767 (1998).
[36] T. A. Jacobson and G. E. Volovik, Phys. Rev. D **58**, 064021 (1998); G. E. Volovik, Phys. Rep. **351**, 195 (2001).
[37] G. E. Volovik, *The Universe in a Helium Droplet*, Vol. 117 (Oxford Unversity Press, Oxford, 2003).
[38] L. J. Garay, J. R. Anglin, J. I. Cirac, and P. Zoller, Phys. Rev. Lett. **85**, 4643 (2000).
[39] J. Steinhauer, Nat. Phys. **10**, 864 (2014); **12**, 959 (2016).
[40] Z.-M. Yu, Y. Yao, and S. A. Yang, Phys. Rev. Lett. **117**, 077202 (2016); M. Udagawa and E. J. Bergholtz, **117**, 086401 (2016); S. Tchoumakov, M. Civelli, and M. O. Goerbig, **117**, 086402 (2016).
[41] We note that the type-I and type-II Dirac/Weyl fermions in these semimetals can be further distinguished from the so-called type-III and type-IV ones with complex frequencies, as discussed in Ref.[49], which is different from the type-III fermions in this work.
[42] See Supplemental Material at http://link.aps.org/supplemental/xxx, for more details about the computation, which include Refs.[4,20,23,24,40,46,50–55].
[43] M. Novello, M. Visser, and G. E. Volovik, *Artificial black holes* (World Scientific, Singapore, 2002).
[44] Ø. Grøn and S. Hervik, *Einstein's general theory of relativity: with modern applications in cosmology* (Springer Science & Business Media, New York, 2007).
[45] S. W. Hawking, Nature **248**, 30 (1974); Commun. Math. Phys. **43**, 199 (1975).
[46] C. Le, S. Qin, X. Wu, X. Dai, P. Fu, C. Fang, and J. Hu, Phys. Rev. B **96**, 115121 (2017).
[47] S. Guan, Z.-M. Yu, Y. Liu, G.-B. Liu, L. Dong, Y. Lu, Y. Yao, and S. A. Yang, npj Quantum Materials **2**, 23 (2017).
[48] R. Schützhold and W. G. Unruh, Phys. Rev. D **66**, 044019 (2002).
[49] J. Nissinen and G. E. Volovik, JETP Lett. **105**, 447 (2017).
[50] G. Kresse and J. Furthmüller, Comput. Mater. Sci. **6**, 15 (1996), `https://www.vasp.at/`.
[51] J. P. Perdew, K. Burke, and M. Ernzerhof, Phys. Rev. Lett. **77**, 3865 (1996).
[52] A. A. Mostofi, J. R. Yates, Y.-S. Lee, I. Souza, D. Vanderbilt, and N. Marzari, Comput. Phys. Commun. **178**, 685 (2008), `http://www.wannier.org/`.
[53] M. P. López Sancho, J. M. López Sancho, and J. Rubio, J. Phys. F **14**, 1205 (1984); **15**, 851 (1985).
[54] A. Jain, S. P. Ong, G. Hautier, W. Chen, W. D. Richards, S. Dacek, S. Cholia, D. Gunter, D. Skinner, G. Ceder, and K. a. Persson, APL Materials **1**, 011002 (2013), `https://materialsproject.org/`.
[55] A. A. Soluyanov and D. Vanderbilt, Phys. Rev. B **83**, 235401 (2011).